



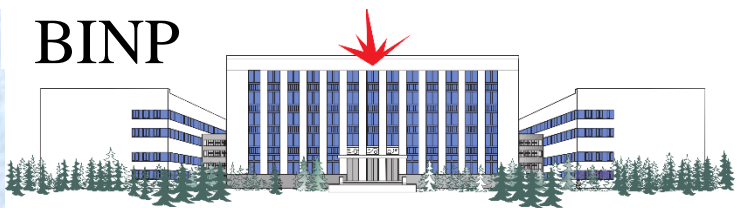
# $e^+e^-$ hadronic cross-sections with SND detector at the VEPP-2000

*On the behalf of SND Collaboration*

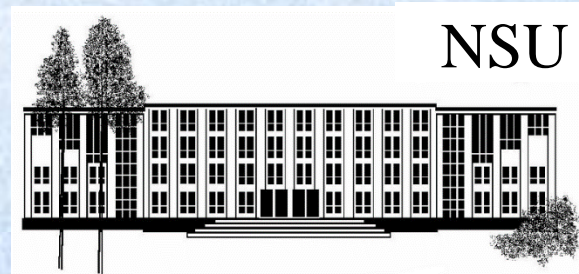
**T.V.Dimova**

30.09.2021

BINP

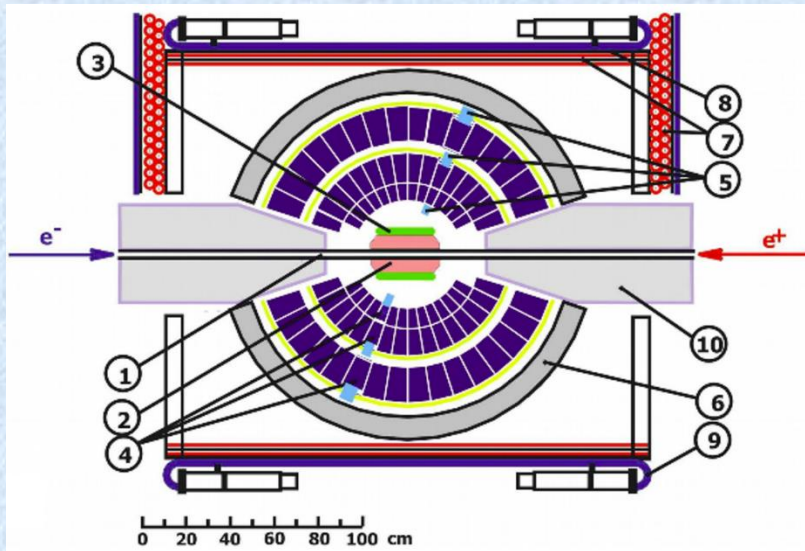


NSU



# SND detector

**NIM A449 (2000) 125-139**



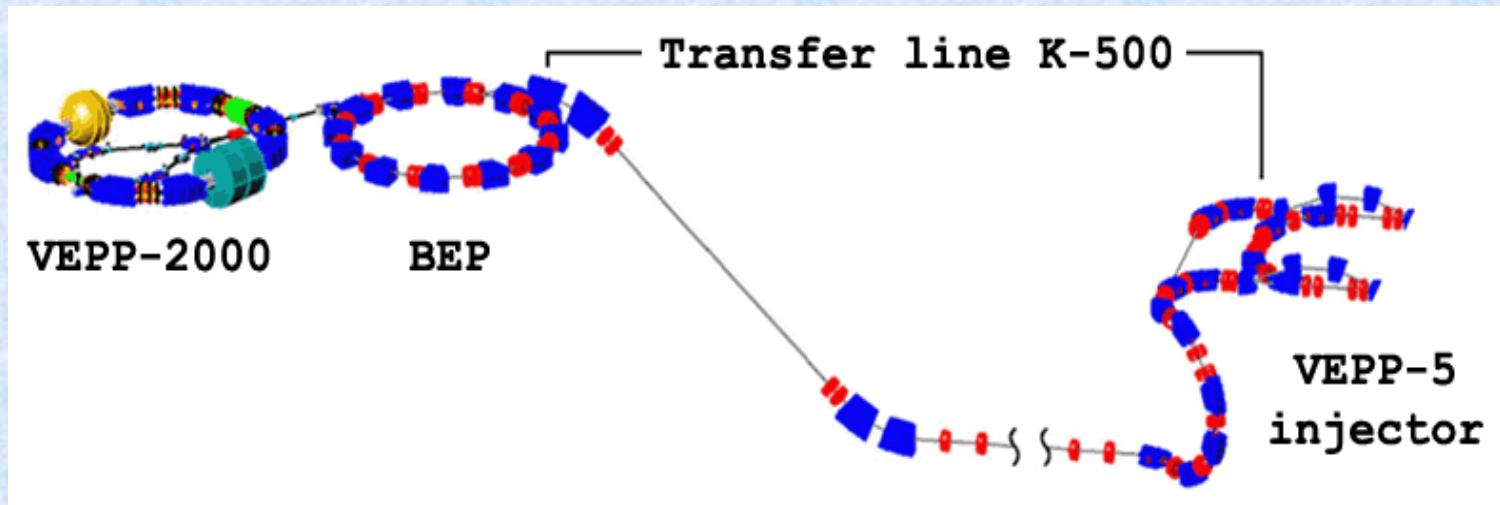
1 – beam pipe, 2 – tracking system, 3 – aerogel Cherenkov counters, 4 – NaI(Tl) crystals, 5 – phototriodes, 6 – iron muon absorber, 7–9 – muon detector, 10 – focusing solenoids.

SND collected data at the VEPP-2M (1996-2000) and VEPP-2000 (2010-2013, 2016-...)

Main physics task of SND is study of all possible processes of  $e^+e^-$  annihilation into hadrons below 2 GeV.

- ❑ The total hadronic cross section, which is calculated as a sum of exclusive cross sections.
- ❑ Study of hadronization (dynamics of exclusive processes):
  - Properties of excited vector mesons of the  $\rho$ ,  $\omega$ ,  $\phi$  families
  - Development of MC event generator for  $e^+e^- \rightarrow$  hadrons below 2 GeV.

# VEPP-2000 $e^+e^-$ collider



## VEPP-2000 parameters:

- c.m. energy  $E=0.3-2.0$  GeV
- circumference – 24.4 m
- round beam optics
- Luminosity at  $E=1.8$  ГэВ  
 $1 \times 10^{32} \text{ cm}^{-2} \text{ sec}^{-1}$  (project)  
 $4 \times 10^{31} \text{ cm}^{-2} \text{ sec}^{-1}$  (achieved)
- Two detectors: SND and CMD-3

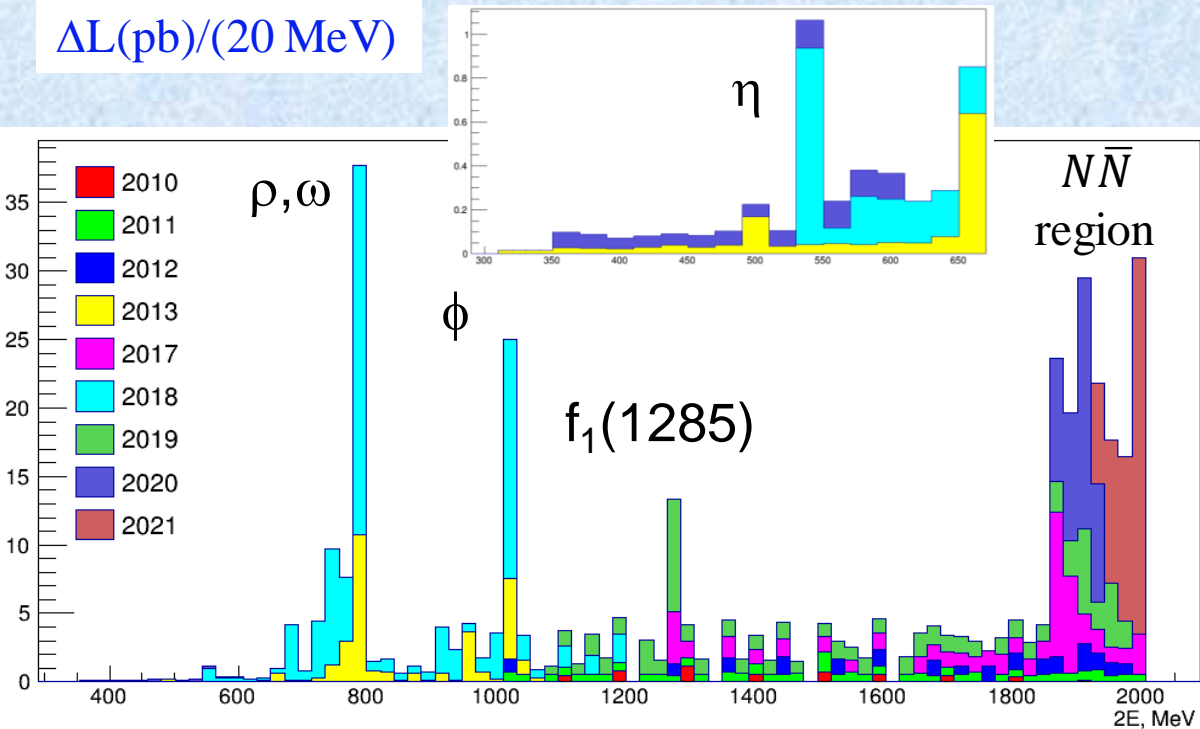
2010-2013 – experiments,  $70 \text{ pb}^{-1}$   
2013-2016 – upgrade, new injector  
2016- ... – experiments,  $300 \text{ pb}^{-1}$

# SND data

	Below $\phi$	Near $\phi$	Above $\phi$
$\mathcal{L}$ , pb $^{-1}$	77	31	259.0
$E_{\text{cm}}$ , GeV	0.30-0.97	0.98-1.05	1.05-2.00

~20 hadronic processes are currently under analysis

$\Delta\mathcal{L}(\text{pb})/(20 \text{ MeV})$



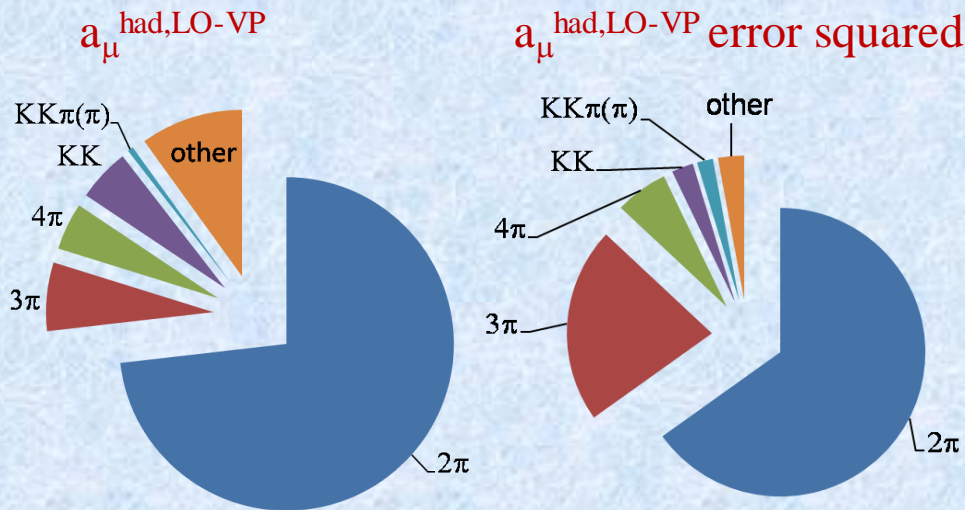
- $e^+e^- \rightarrow \pi^+\pi^-$
- $e^+e^- \rightarrow n\bar{n}$
- $e^+e^- \rightarrow p\bar{p}$
- $e^+e^- \rightarrow \pi^+\pi^-\pi^0$
- $e^+e^- \rightarrow K^+K^-\pi^0$
- $e^+e^- \rightarrow \pi^0\eta\gamma$
- $e^+e^- \rightarrow \eta\eta\gamma$
- $e^+e^- \rightarrow \omega\pi^0 \rightarrow \pi^+\pi^-\pi^0\pi^0$

30.09.2021

TAU2021

$$e^+e^- \rightarrow \pi^+\pi^-$$

The process  $e^+e^- \rightarrow \pi^+\pi^-$  gives the largest contribution into  $a_\mu^{\text{had,LO-VP}}$  and its error.



- ✓ There are many measurements of the  $e^+e^- \rightarrow \pi^+\pi^-$  process, some of them have systematic uncertainty less than 1%.
- ✓ The most precise measurements with a systematic uncertainty of about 0.6% were done by BABAR and KLOE using the ISR technique.
- ✓ However, the difference between the BABAR and KLOE cross sections reaches several %.

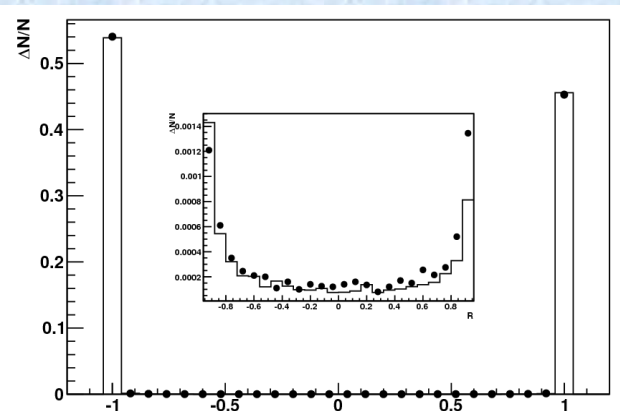
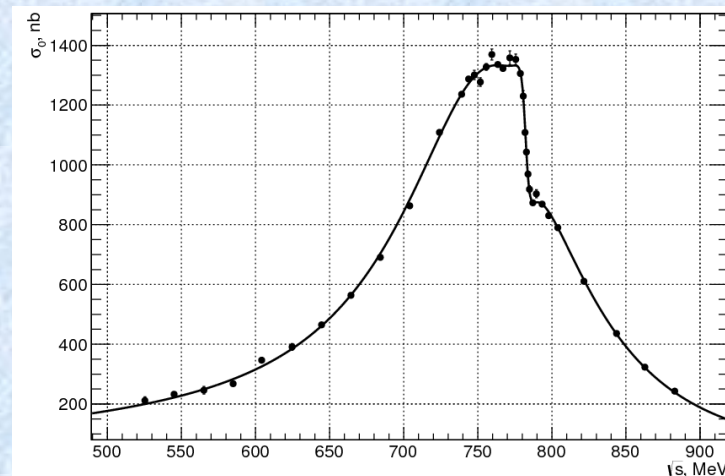
Experiments at VEPP-2000 use direct scan approach and may provide fully independent measurements with a sub-% accuracy.

$$e^+e^- \rightarrow \pi^+\pi^-$$

JHEP 01,113 (2021)

$e/\pi$  separation parameter

The analysis is based on 4.7 pb<sup>-1</sup> data recorded in 2013 (1/10 full SND data set)



Systematic uncertainty on the cross section (%)

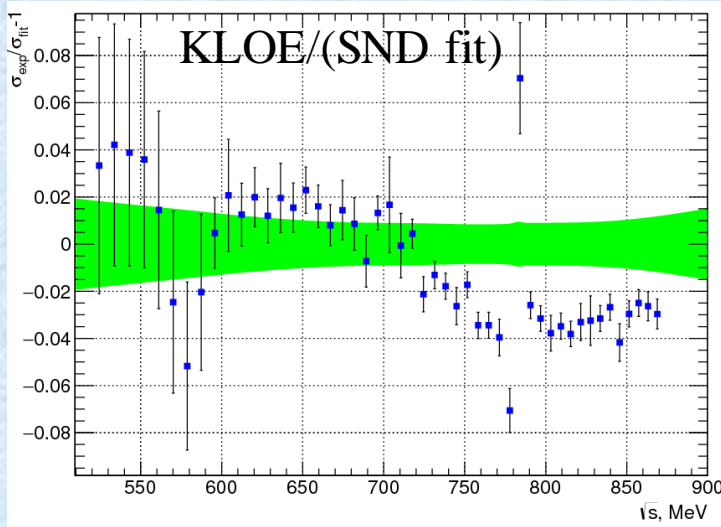
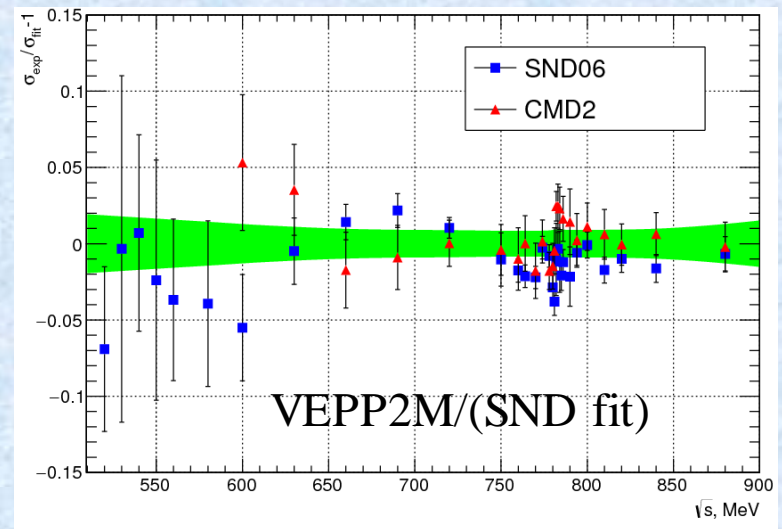
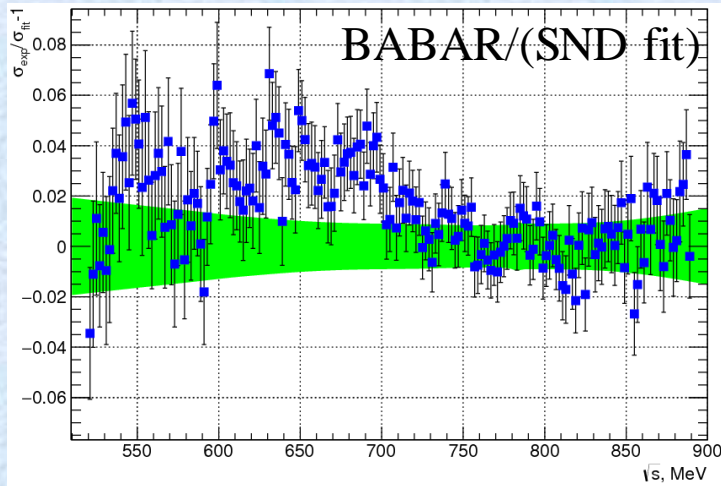
Source	< 0.6 GeV	0.6 - 0.9 GeV
Trigger	0.5	0.5
Selection criteria	0.6	0.6
$e/\pi$ separation	0.5	0.1
Nucl. interaction	0.2	0.2
Theory	0.2	0.2
<b>Total</b>	<b>0.9</b>	<b>0.8</b>

	SND @ VEPP-2000	SND @ VEPP-2M	PDG
$M_\rho$ , MeV	$775.3 \pm 0.5 \pm 0.6$	$775.6 \pm 0.4 \pm 0.5$	$775.3 \pm 0.3$
$\Gamma_\rho$ , MeV	$145.6 \pm 0.6 \pm 0.8$	$146.1 \pm 0.8 \pm 1.5$	$147.8 \pm 0.9$
$B_{\rho ee} \times 10^5$	$4.89 \pm 0.2 \pm 0.4$	$4.88 \pm 0.2 \pm 0.6$	$4.72 \pm 0.5$
$B_{\omega\pi\pi}$ , %	$1.77 \pm 0.08 \pm 0.02$	$1.66 \pm 0.08 \pm 0.05$	$1.53 \pm 0.06$

30.09.2021

TAU2021

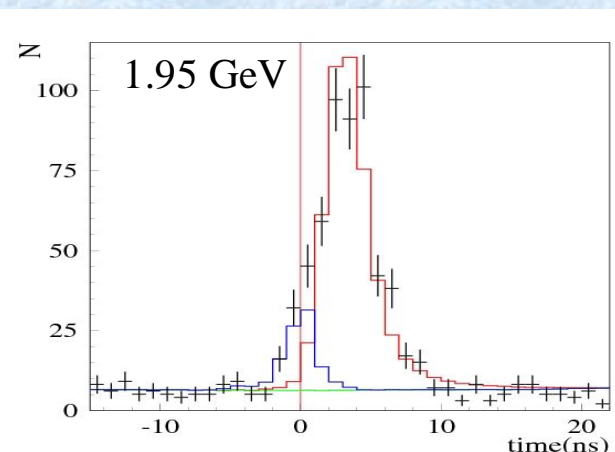
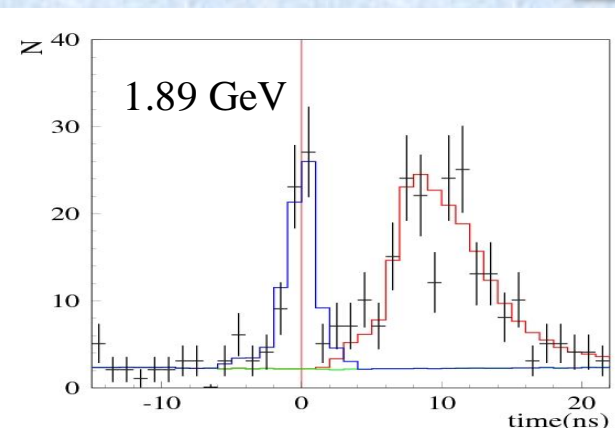
$$e^+e^- \rightarrow \pi^+\pi^-$$



$0.53 < \sqrt{s} < 0.88 \text{ GeV}$

	$a_\mu(\pi^+\pi^-) \times 10^{10}$
SND & VEPP-2000	$409.8 \pm 1.4 \pm 3.9$
SND & VEPP-2M	$406.5 \pm 1.7 \pm 5.3$
BABAR	$413.6 \pm 2.0 \pm 2.3$
KLOE	$403.4 \pm 0.7 \pm 2.5$

# $e^+e^- \rightarrow n\bar{n}$

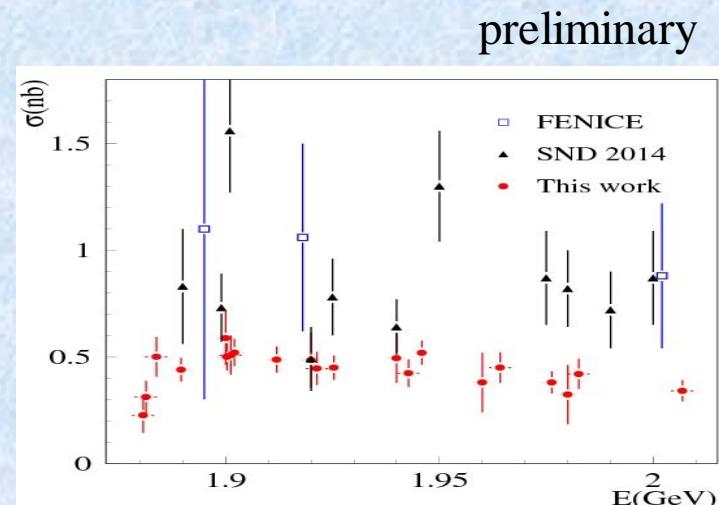


➤ This process near threshold was previously measured by FENICE and SND using the 2011-2012 dataset.

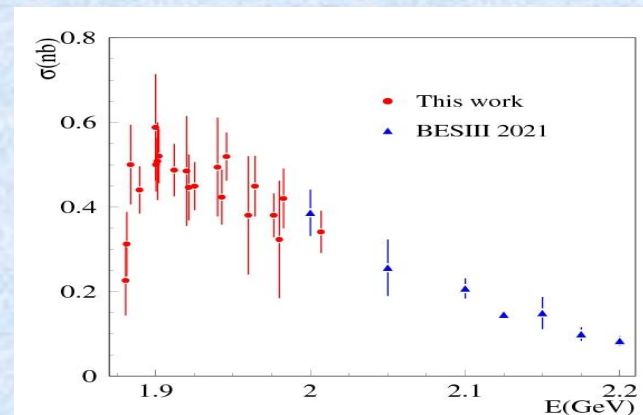
➤ The new measurement is based on the 2017, 2019 data ( $38 \text{ pb}^{-1}$ ) and uses time measurement in the calorimeter.

➤ The time distribution is fitted by a sum of distributions for signal, cosmic background, and beam +  $e^+e^-$  annihilation background.

➤ Our new result is lower than the previous. The main reasons are underestimated beam background and incorrect MC simulation.



The systematic uncertainty is 10%



preliminary



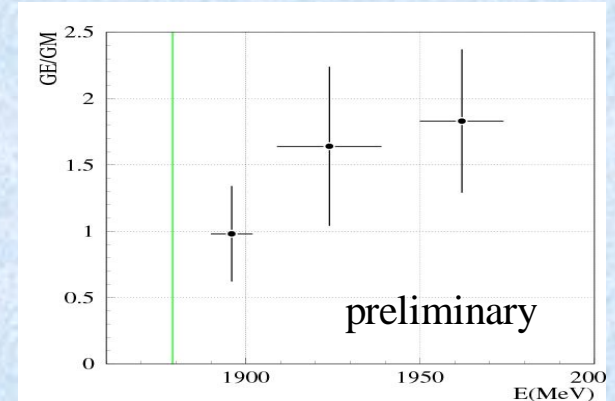
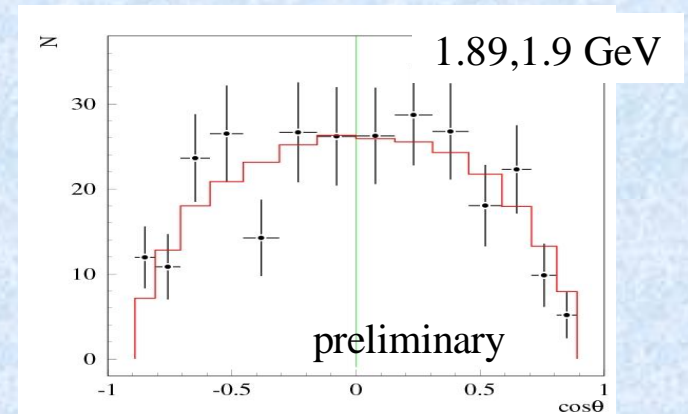
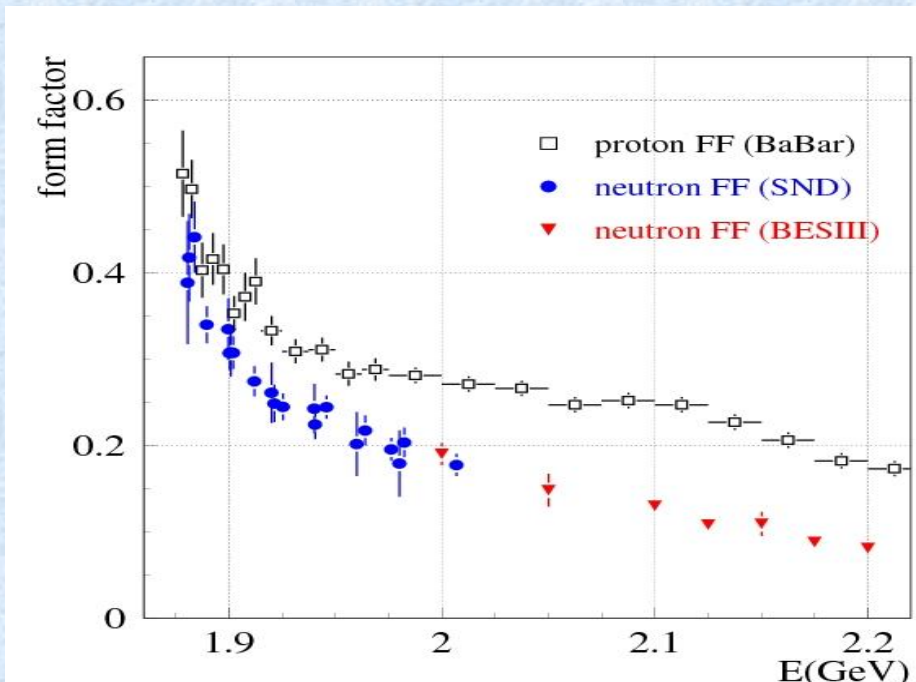
# Neutron electromagnetic form factors

From the measured cross section, we determine effective form factor

$$|F|^2 = \frac{|G_M|^2 + \frac{2m_n^2}{s}|G_E|^2}{1 + \frac{2m_n^2}{s}}$$

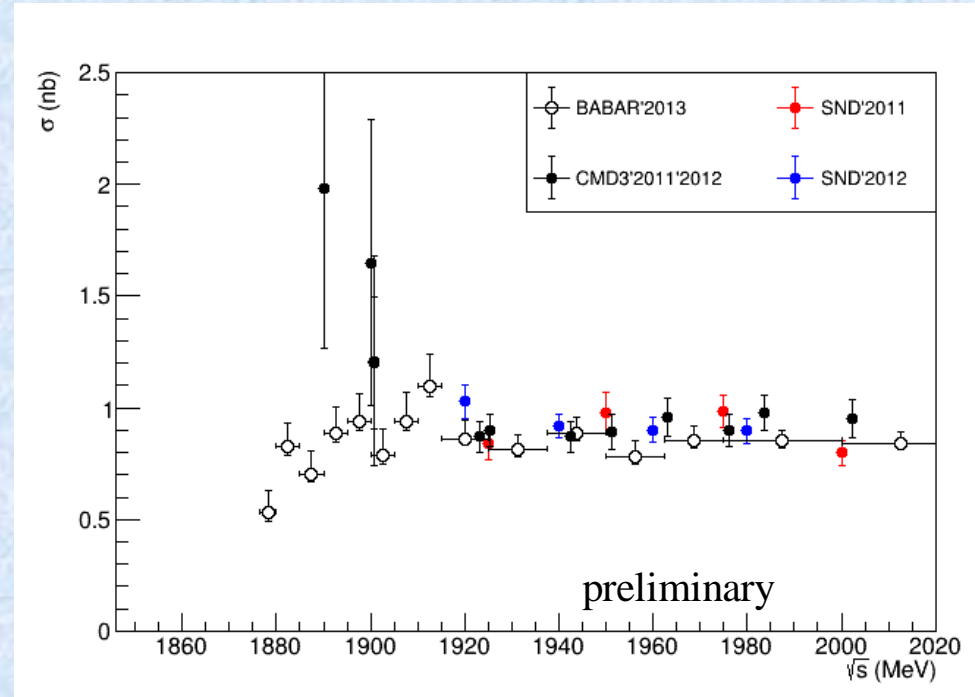
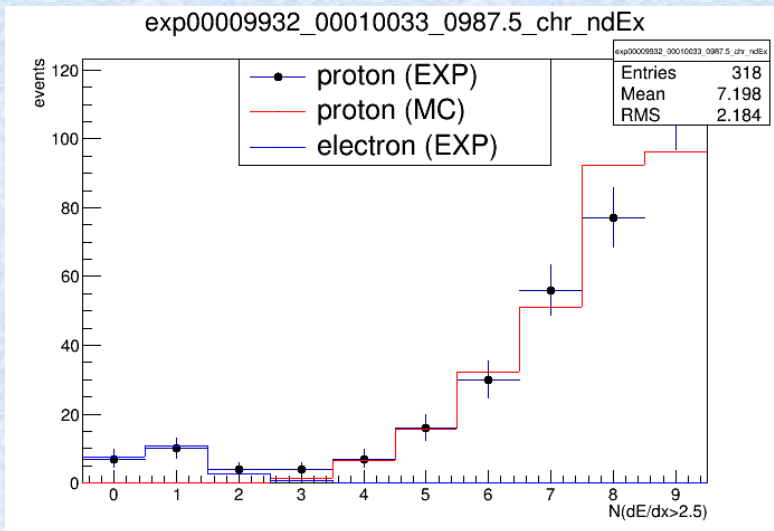
$$\sigma(e^+e^- \rightarrow n\bar{n}) = \frac{\alpha^2\beta}{4s} \left[ |G_M|^2(1 + \cos^2\theta) + \frac{4m_n^2}{s}|G_E|^2\sin^2\theta \right]$$

From analysis of the antineutron polar-angle distribution we determine the ratio of the form factors



$$e^+e^- \rightarrow p\bar{p}$$

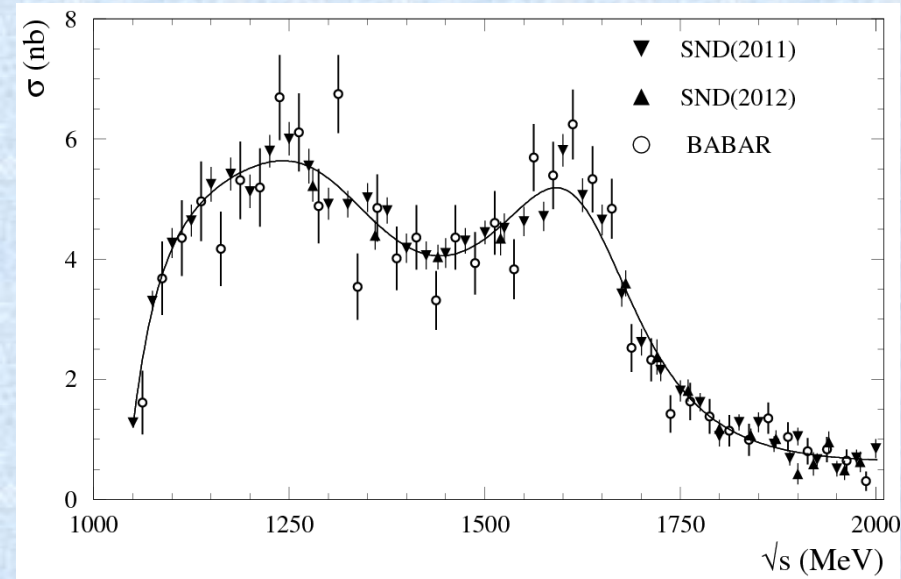
- This process near threshold was previously measured by BABAR and CMD3.
- Our measurement is based on the 2011-2012 data and uses energy deposition measurement in the drift chamber.



The number of DC layers with dEdx exceeding 2.5\*dEdx of the electron

# $e^+e^- \rightarrow \pi^+\pi^-\pi^0$ cross section

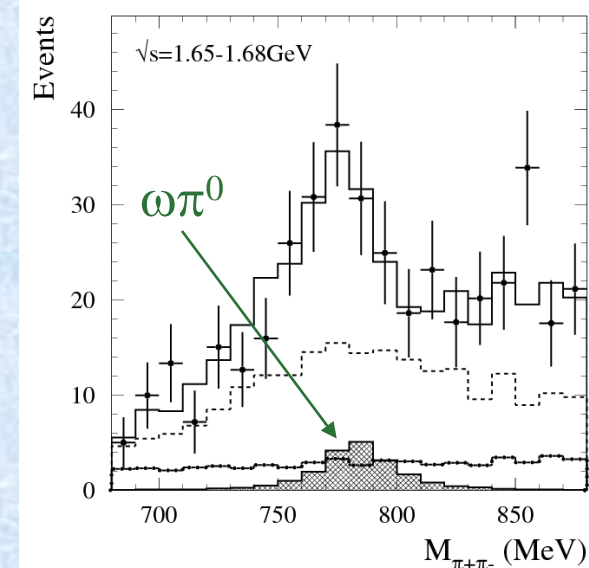
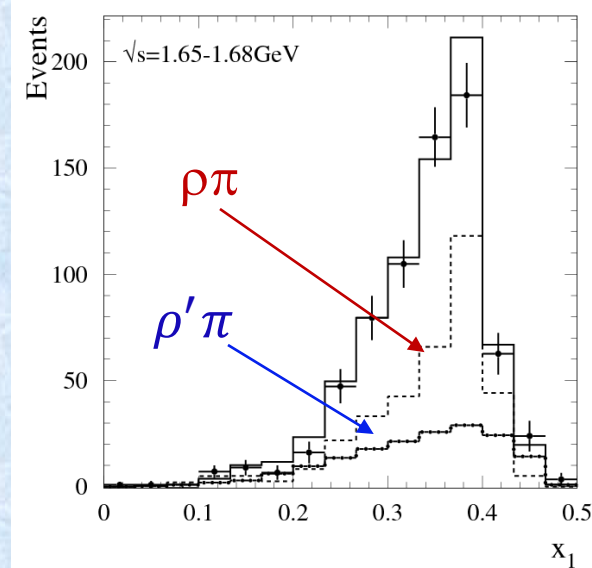
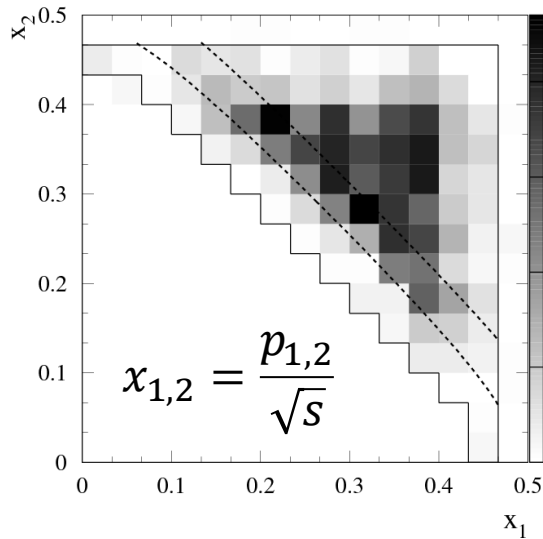
EPJ C **80** (2020) 993



- ✓ Both SND measurements are consistent with each other and with the the BABAR measurement.
- ✓ Two peaks in the cross section corresponds to the  $\omega' \equiv \omega(1420)$  and  $\omega'' \equiv \omega(1650)$  resonances.
- ✓ The systematic uncertainty on the cross section is 4.4%.

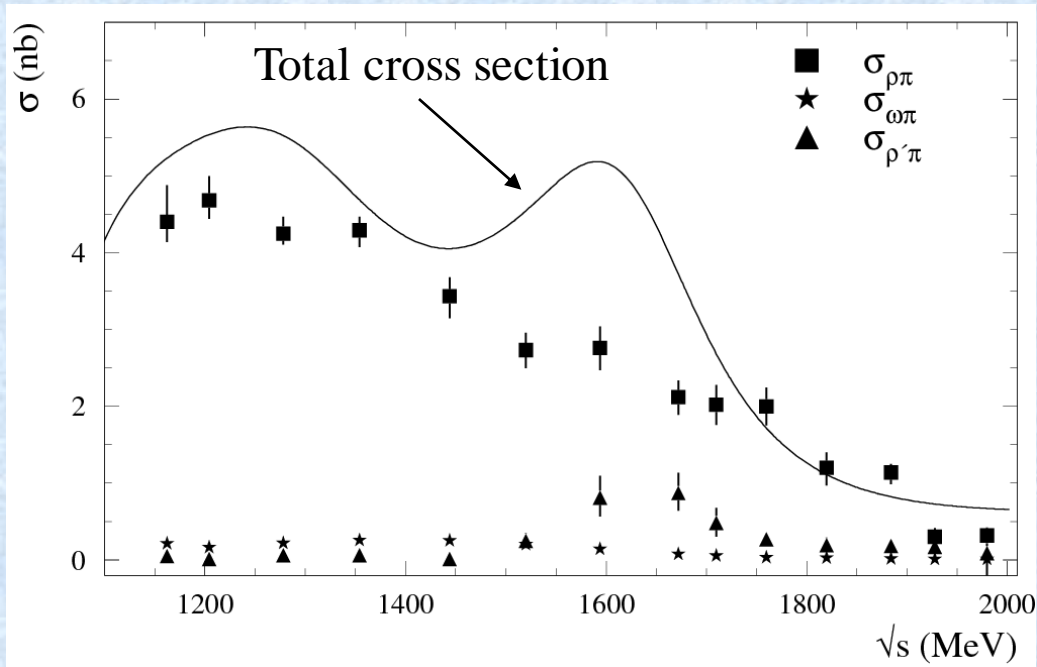
The previous SND measurement [J. Exp. Theor. Phys. 121, 27 (2015)] is based on 2011 data set. The 2012 data set has been added.

# $e^+e^- \rightarrow \pi^+\pi^-\pi^0$ dynamics



- We analyze the two-dimensional distribution of the charged-pion momenta and the  $\pi^+\pi^-$  mass spectrum.
- These distributions are fitted with a model including the  $\rho\pi$ ,  $\rho'\pi \equiv \rho(1450)\pi$ , and  $\omega\pi^0$  states.
- A significant fraction of the  $\rho'\pi$  intermediate state is observed in the energy region 1.55-1.75 GeV.

# $e^+e^- \rightarrow \pi^+\pi^-\pi^0$ dynamics

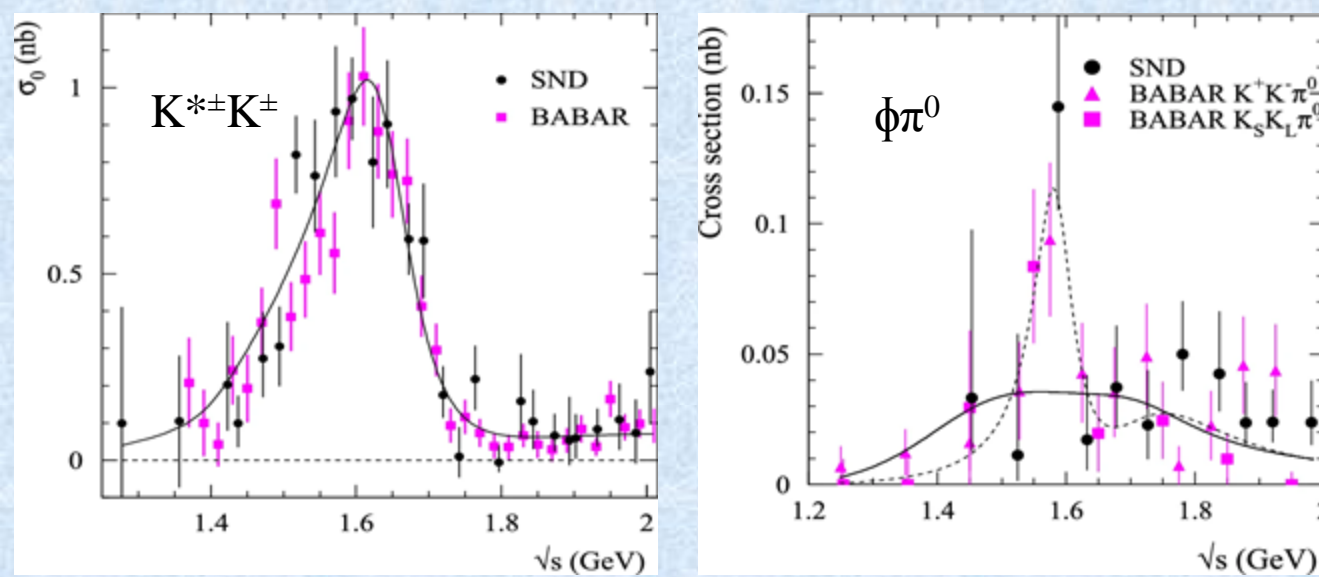


- ✓ The isovector intermediate state  $\omega\pi^0$  gives sizable (up to 20%) contribution to the  $e^+e^- \rightarrow \pi^+\pi^-\pi^0$  cross section.
- ✓ The cross section for the intermediate state  $\rho'\pi$  differs significantly from zero in the range 1.55 - 1.75 GeV, where the resonance  $\omega''$  is located.
- ✓ In the  $\rho\pi$  cross section the resonance structure near 1650 MeV is not seen.

We conclude that the  $\rho'\pi$  intermediate state gives a significant contribution to the decay  $\omega'' \rightarrow \pi^+\pi^-\pi^0$ , and that the  $\omega' \rightarrow \pi^+\pi^-\pi^0$  decay is dominated by the  $\rho\pi$  intermediate state.

$$e^+e^- \rightarrow K^+K^-\pi^0$$

EPJ C **80** (2020) 1139

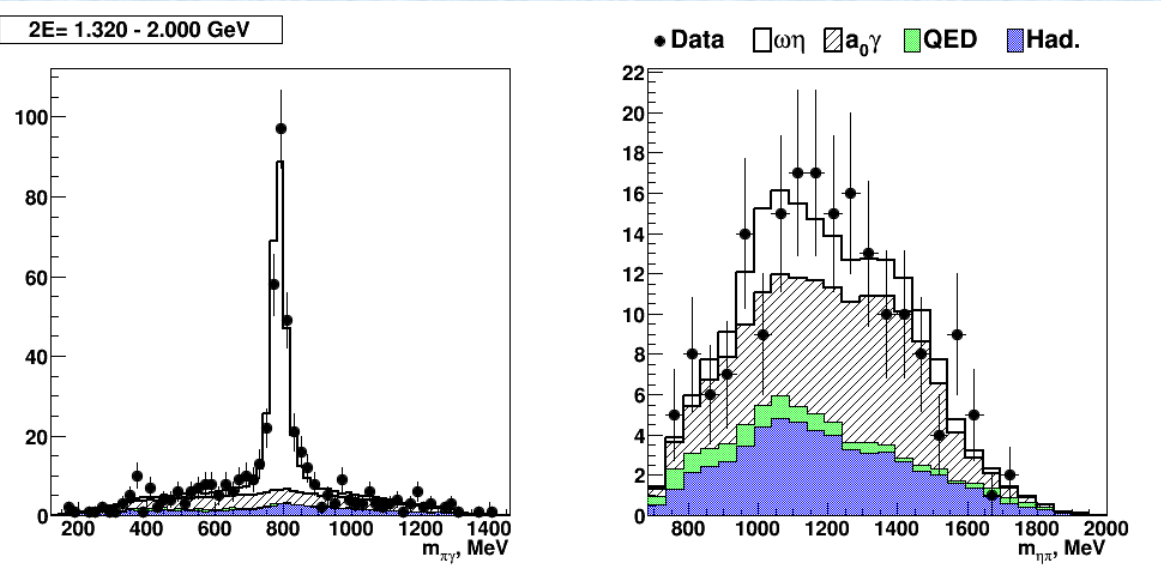


- The analysis is based on 26  $\text{pb}^{-1}$  data recorded in the c.m. energy range 1.27 – 2 GeV.
- The cross sections for the  $K^{*\pm}K^\mp$  and  $\phi\pi^0$  intermediate states are measured separately.
- The  $e^+e^- \rightarrow K^{*\pm}K^\mp$  cross section is dominated by the  $\phi' \equiv \phi(1680)$  resonance.

The isovector process  $e^+e^- \rightarrow \phi\pi^0$  is suppressed by the Okubo-Zweig-Iizuka (OZI) rule. Three measurements of the cross section are fitted simultaneously. The fit by a sum of the  $\rho'$  and  $\rho''$  contributions cannot describe data near 1.6 GeV. The inclusion of an unknown resonance with  $m=1585\pm 15$  MeV and  $\Gamma=75\pm 30$  MeV improves fit. The significance of the structure is about  $3\sigma$ .

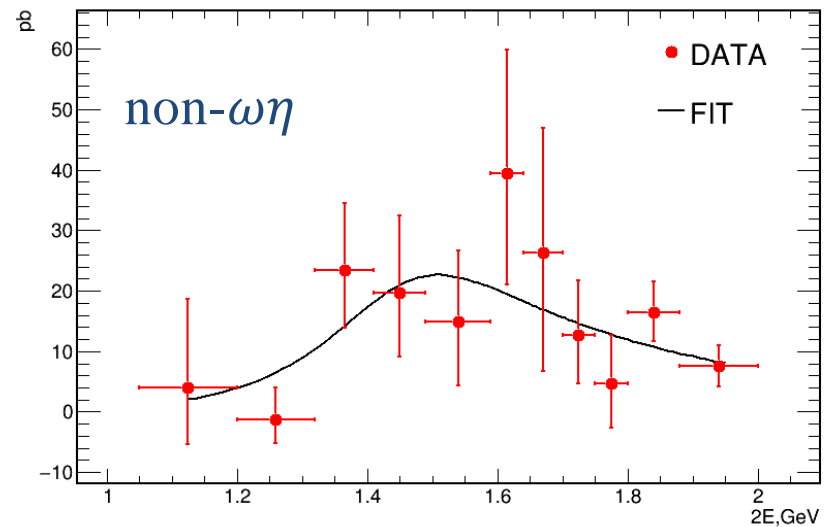
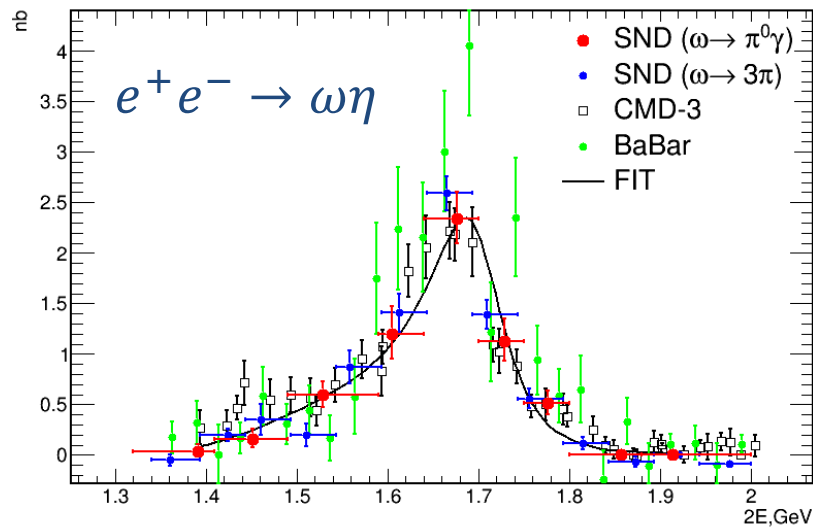
$$e^+e^- \rightarrow \eta\pi^0\gamma$$

- ✓ There is a significant contribution of the  $\omega\eta$  intermediate state, which is seen as a peak in the  $\pi^0\gamma$  mass distribution.
- ✓ The non- $\omega\eta$  signal is observed with significance of  $5.6\sigma$ . It has a wide  $\eta\pi^0$  mass distribution and may arise from the processes  $e^+e^- \rightarrow a_0(1450)\gamma$  and  $a_2(1320)\gamma$ .



- The process  $e^+e^- \rightarrow \eta\pi^0\gamma$  above 1.05 GeV is studied for the first time.
- Data set with  $\mathcal{L}\approx 100 \text{ pb}^{-1}$  recorded in 2010-2012 and 2017
- The five-photon final state is used.

$$e^+e^- \rightarrow \eta\pi^0\gamma$$

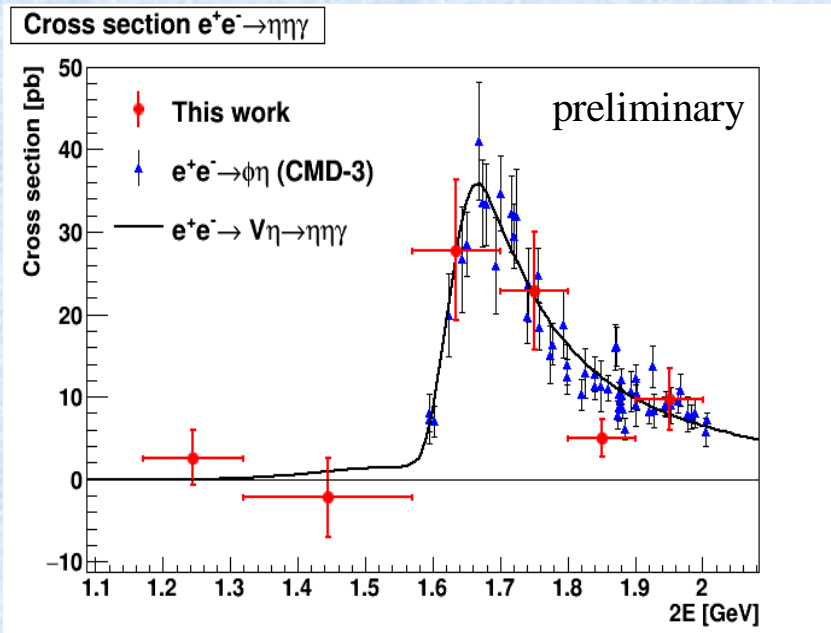


The measured  $e^+e^- \rightarrow \omega\eta$  cross section is in good agreement with the SND and CMD-3 measurements in the  $\omega \rightarrow \pi^+\pi^-\pi^0$  decay mode.

The non-VP  $e^+e^- \rightarrow \eta\pi^0\gamma$  process is observed with significance of  $5.6\sigma$ .  
**This is the first measurement of this cross section.**



# $e^+e^- \rightarrow \eta\eta\gamma$



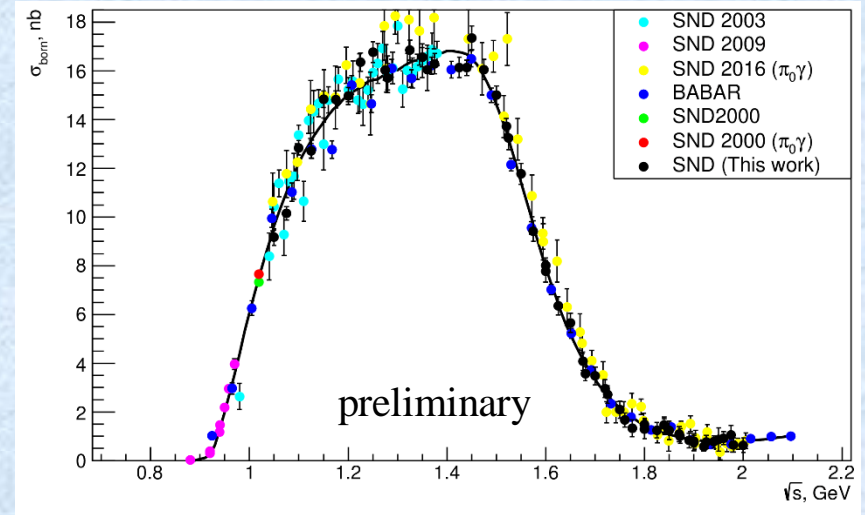
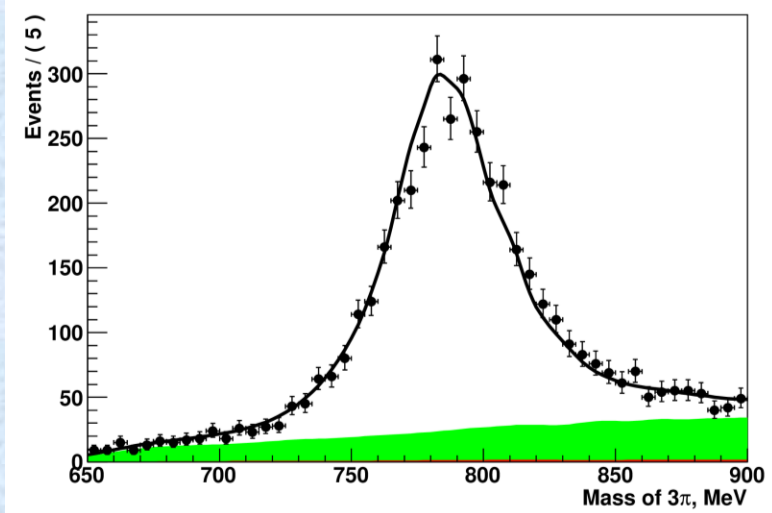
- The  $e^+e^- \rightarrow \eta\eta\gamma$  cross section is measured for the first time in the energy range 1.17 – 2.0 GeV.
- The main intermediate state is  $\phi\eta$ .
- The measured cross section is consistent with CMD-3 result on  $e^+e^- \rightarrow \phi\eta$ ,  $\phi \rightarrow K^+K^-$ .
- The contribution from intermediate states other than  $\phi\eta$  is not seen.

Upper limits on possible contribution of radiative intermediate states ( $f_0(1500)\gamma$ ,  $f_2^*(1525)\gamma$ ) is set.

preliminary

2E, GeV	95% CL Upper limit, pb
1.17-1.32	9
1.32-1.57	5
1.57-1.80	11
1.80-2.00	4

$$e^+e^- \rightarrow \omega\pi^0 \rightarrow \pi^+\pi^-\pi^0\pi^0$$



- The analysis is based on  $35 \text{ pb}^{-1}$  data collected in 2011 – 2012.
- The measurement of the  $e^+e^- \rightarrow \omega\pi^0$  process is the first step in the study of the  $e^+e^- \rightarrow \pi^+\pi^-\pi^0\pi^0$  reaction.
- Allows to study all sources of systematic uncertainties
- The  $\omega\pi^0$  contribution is separated from other intermediate states ( $a_1\pi$ ,  $\rho^+\rho^-$ , ...) by fitting the  $\pi^+\pi^-\pi^0$  invariant-mass spectrum in the range 650 – 900 MeV.

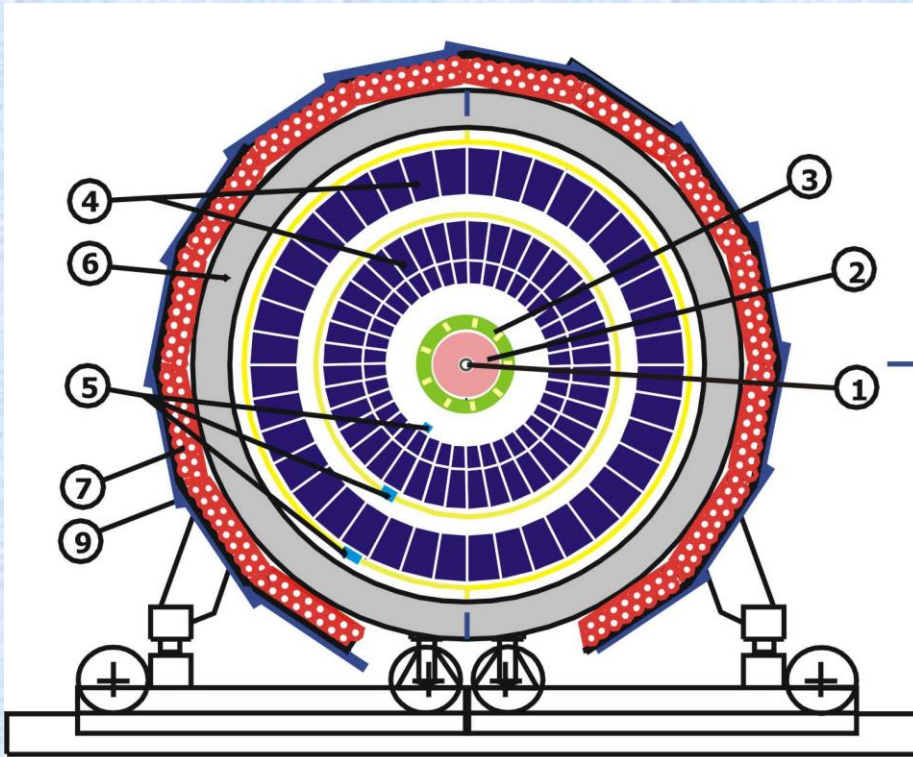
- The  $\omega\pi^0$  cross section measured with the restriction  $M(3\pi) < 0.9 \text{ GeV}$  is expected to be independent of the model for the  $\omega$  line shape.
- The measured cross section is in agreement with previous measurements but has better accuracy.
- The cross section is fitted with the VMD model including three  $\rho$ -like states

# Summary

- ✓ The SND detector accumulated  $370 \text{ pb}^{-1}$  of integrated luminosity in the energy range  $0.3 - 2 \text{ GeV}$ .
- ✓ The  $e^+e^- \rightarrow \pi^+\pi^-$  cross section has been measured in the energy range  $0.53-0.88 \text{ GeV}$  with a systematic uncertainty **better than 1%**.
- ✓ The accuracy of the  $e^+e^- \rightarrow n\bar{n}$  measurement has been significantly improved.
- ✓ The preliminary results on the  $e^+e^- \rightarrow p\bar{p}$  cross section has been obtained.
- ✓ The dynamics of the process  $e^+e^- \rightarrow \pi^+\pi^-\pi^0$  has been studied in the energy range  $1.15-2.0 \text{ GeV}$ .
- ✓ The process  $e^+e^- \rightarrow K^+K^-\pi^0$  has been studied in the  $K^{*\pm}K^{\mp}$  and  $\phi\pi^0$  intermediate states.
- ✓ Rare radiative processes  $e^+e^- \rightarrow \eta\pi^0\gamma$  and  $\eta\eta\gamma$  have been measured in the energy range  $1.05-2 \text{ GeV}$ .
- ✓ The most precise measurement of the  $e^+e^- \rightarrow \omega\pi^0 \rightarrow \pi^+\pi^-\pi^0\pi^0$  cross section has been performed.

# Backup slides

# SND detector



1 – beam pipe, 2 – tracking system, 3 – aerogel Cherenkov counters, 4 – NaI(Tl) crystals, 5 – phototriodes, 6 – iron muon absorber, 7–9 – muon detector, 10 – focusing solenoids.

## Calorimeter

Thickness	$13.5 X_0$
Acceptance	$0.95 \times 4\pi$
Energy resolution	$\frac{\sigma_E}{E} = \frac{0.042}{\sqrt[4]{E[GeV]}}$
Angular resolution	$\sigma_{\phi, \theta} = \frac{0.82^\circ}{\sqrt[4]{E[GeV]}} \oplus 0.63^\circ$

## Tracking system

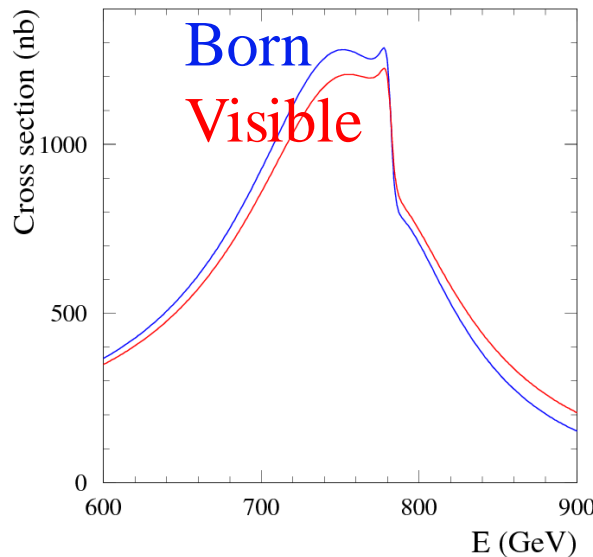
Acceptance (9 layers)	$0.94 \times 4\pi$
Angular resolution	$\sigma_\phi = 0.55^\circ, \sigma_\theta = 1.2^\circ$
Vertex resolution	$\sigma_R = 0.12cm,$ $\sigma_Z = 0.45cm$

## Aerogel counters

K/ $\pi$ separation	$E < 1 \text{ GeV}$
---------------------	---------------------

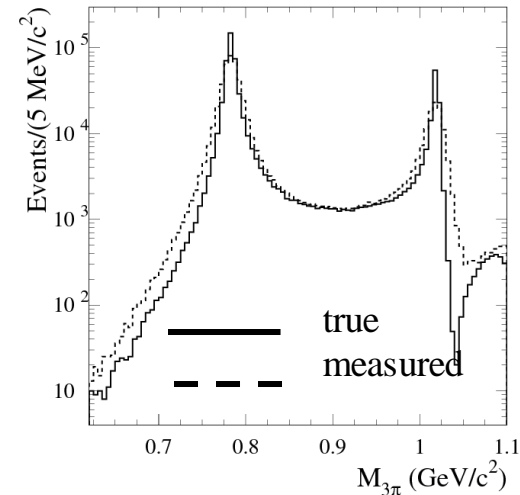
# Direct scan vs ISR

Energy scan  $e^+e^- \rightarrow \pi^+\pi^-$



- ❑ In both methods, the integral equation should be resolved to obtain the Born cross section.
- ❑ The function  $W(x,E)$  is well known theoretically
- ❑ The resolution function  $R(M_m, M_t)$  is determined using simulation and tested at narrow resonances. The data –MC difference in the tails of the resolution is hard to be tested.

ISR  $e^+e^- \rightarrow \pi^+\pi^-\pi^0\gamma$



$$\sigma_{vis} = \int_0^{x_m} W(x, E) \sigma_b(\sqrt{E(1-x)}) dx$$

$$\frac{dN}{dM_m} = \int_0^\infty R(M_m, M_t) \frac{dN}{dM_t} dM_t$$